nature climate change

SUPPLEMENTARY INFORMATION

DOI: 10.1038/NCLIMATE1530

Twenty-first-century projections of North Atlantic tropical storms from CMIP5 models

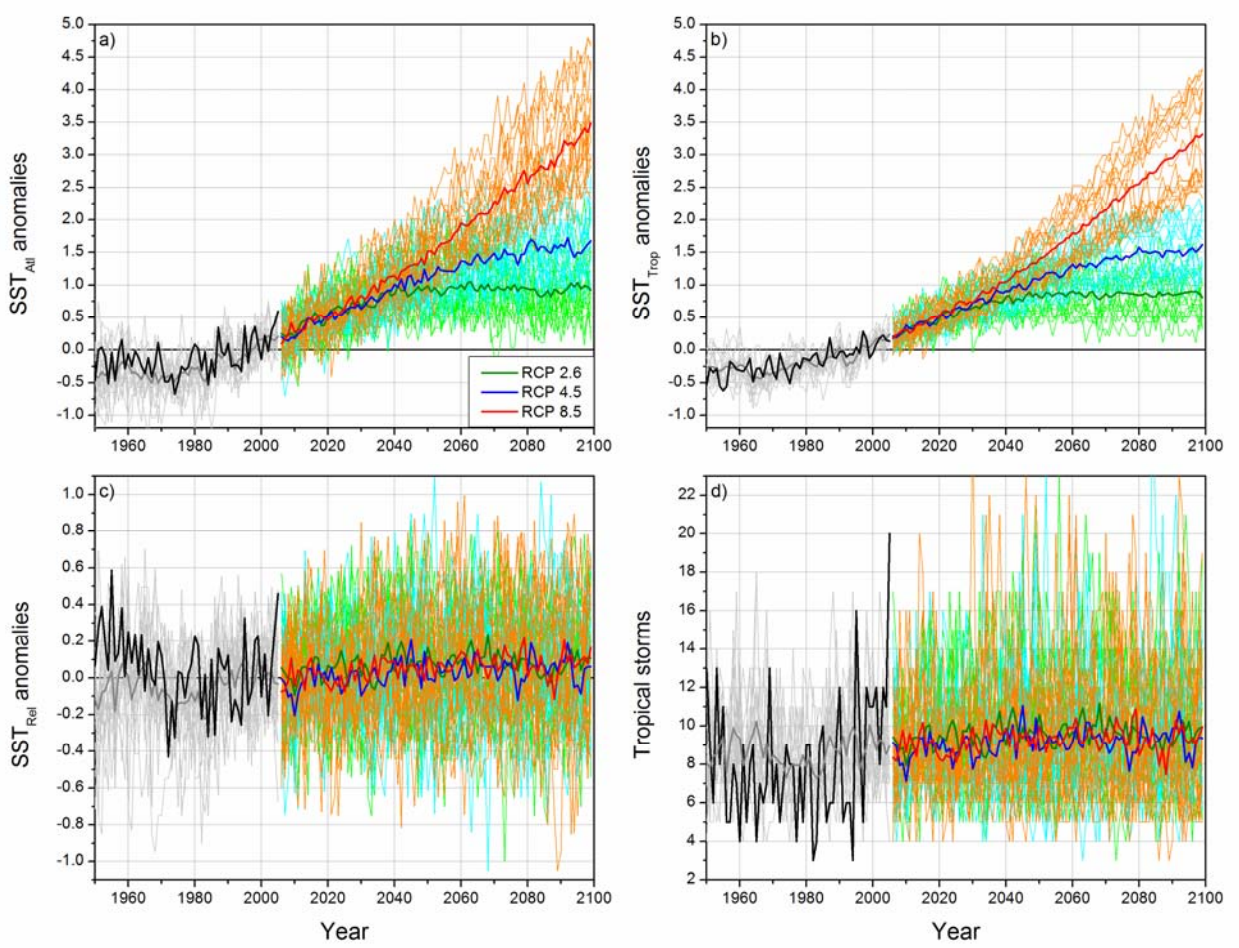

SUPPLEMENTARY FIGURE 1. Annual tropical Atlantic SST anomalies (top left panel), tropical mean SST anomalies (top right panel), relative SST anomalies (defined as tropical Atlantic minus tropical mean SSTs; bottom left panel), and tropical storm count (bottom right panel) projections from 17 global climate models under the CMIP5 for three scenarios (RCP 2.6, RPC 4.5, and RCP 8.5). The solid thicker lines represent the mean from each of the three scenarios. The light grey lines from 1950 to 2005 describe the historical runs for the 17 global climate models, while the solid black lines the observations (National Oceanic and Atmospheric Administration (NOAA) Extended Reconstructed SST (ERSSTv3b; Smith et al. 2008) for the SST, and the Hurricane Database (HURDAT; Jarvinen et al. 1984, McAdie et al. 2009, Landsea et al. 2010) data for the tropical storms). The SST anomalies are computed over June-November with respect to 1986-2005; seasonal tropical storm frequency is derived with the statistical model of Villarini et al. (2010).

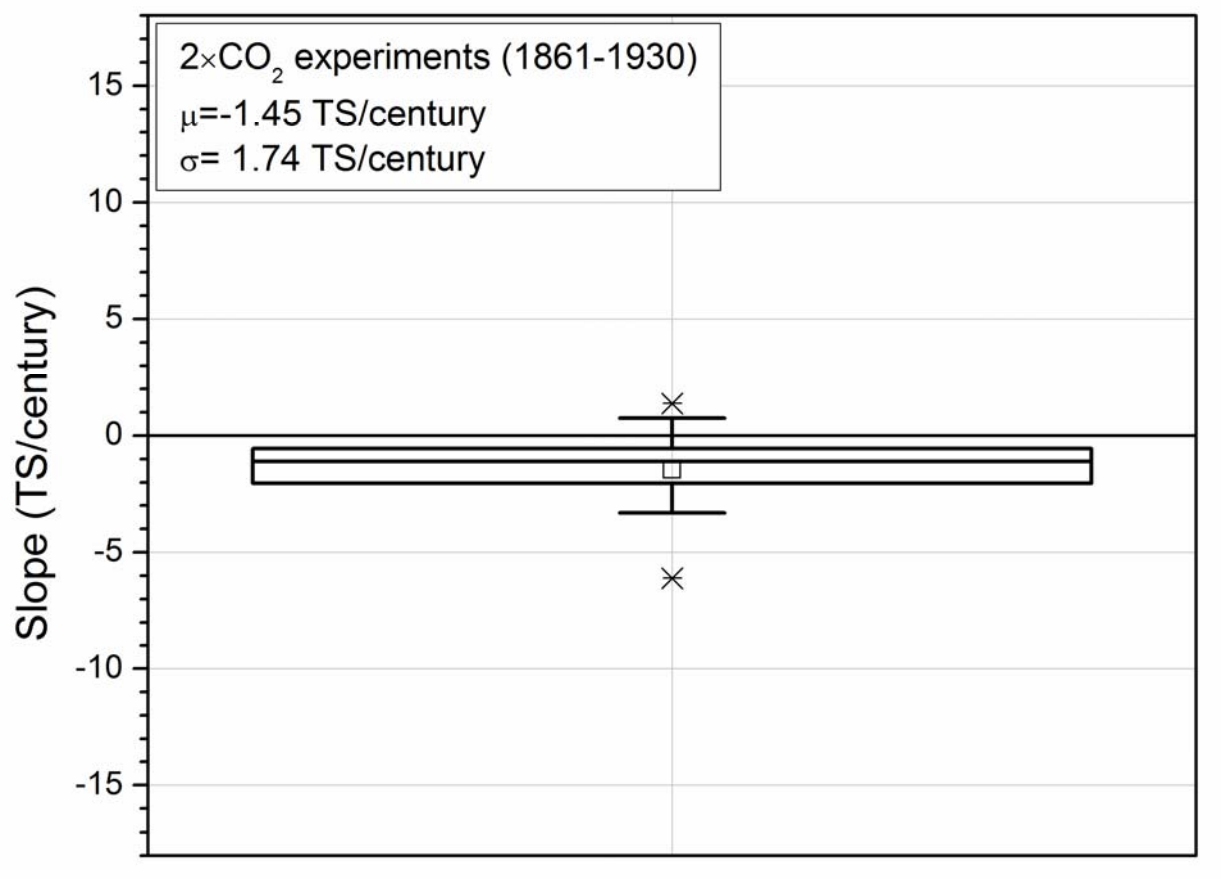

SUPPLEMENTARY FIGURE 2. Slopes of the regression lines for the period 1861-1930 for 16 global climate models and $2\times CO_2$ experiment. In the box plots, the crosses represent the minimum and maximum values, the limits of the whiskers represent the 10^{th} and 90^{th} percentiles, the limits of the boxes represent the 25^{th} and 75^{th} percentiles, and the horizontal lines and the squares inside the boxes are the median and the mean, respectively.

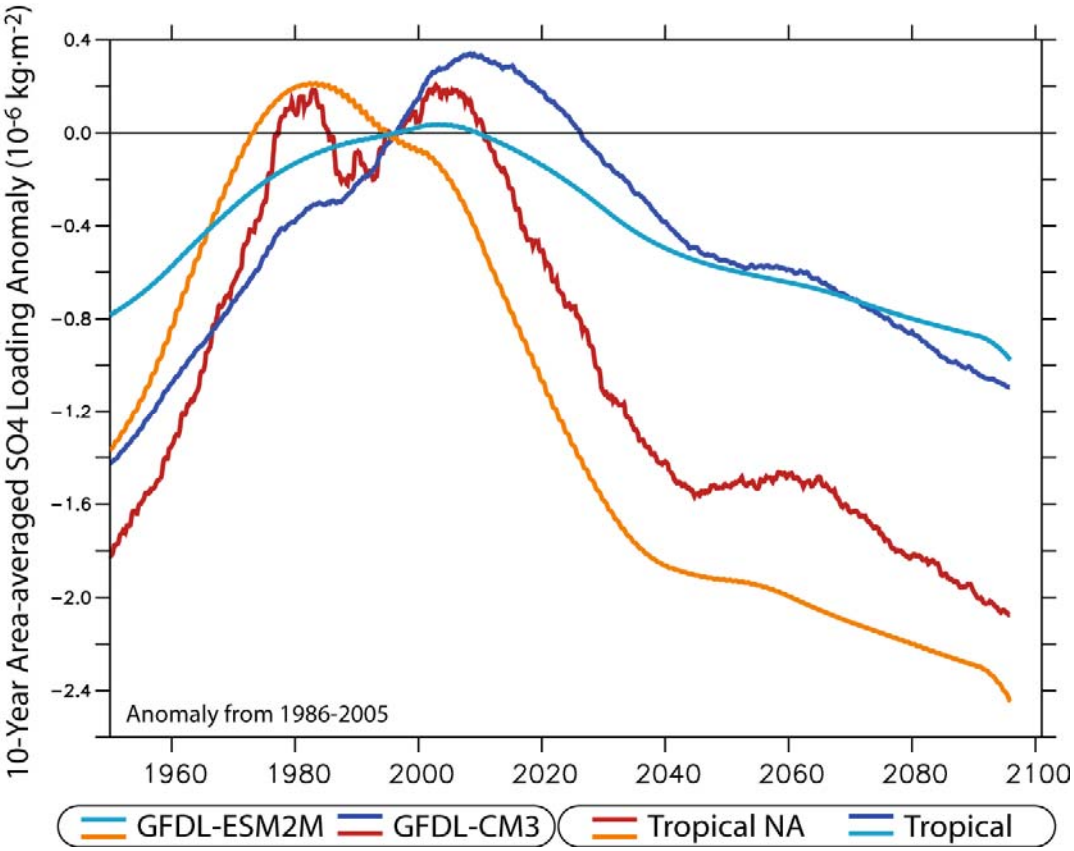

SUPPLEMENTARY FIGURE 3. Time series plot of the sulfate aerosol loading from two of the GFDL models under RCP2.6 (CM3 and ESM2M – the aerosols in ESM2G are identical to those in ESM2M) over the tropical North Atlantic Ocean (red/orange lines) and global tropical oceans (blue lines). Although focusing solely on local sulfate aerosol loading is not sufficient to assess the net impact of sulfates, much less that of the entire suite of aerosol species, this figure provides perspective on changes in the aerosol forcing in these scenarios. Though there are some differences between these models, there are broad consistencies between CM3 and ESM2M. Both in CM3 and ESM2M Tropical Atlantic sulfate loading increases quite rapidly (more than in the tropical-mean) through the early-1980s, after which it either begins to decrease (ESM2M) or stalls (CM3) – as tropical-mean sulfate loading continues to grow. Through the mid-2030s, the sulfate loading in the tropical Atlantic decreases rapidly in both models, while the tropical-mean sulfate loading decreases more slowly. Following the 2040s, the change in tropical-mean and tropical Atlantic sulfate loading is similar. Therefore, to the extent that local aerosol loading is an indicator of the response of local SST (which is not the case in detail), this evolution suggests a period where aerosols acted to cool the Atlantic relative to the tropics up to the 1980s, a period where the tropics began to cool relative to the Atlantic after that, and a rapid warming of the Atlantic relative to the tropics through the mid-21st century. Therefore, the timing of the model response of relative SST and tropical storm frequency is qualitatively consistent with the evolution of sulfate aerosols. However, the net impact of aerosols (even only sulfate) could be

more complex than indicated by this figure, and is best diagnosed within the global circulation models by running experiments where one forcing agent is left out (see Supplemental Figure 4).

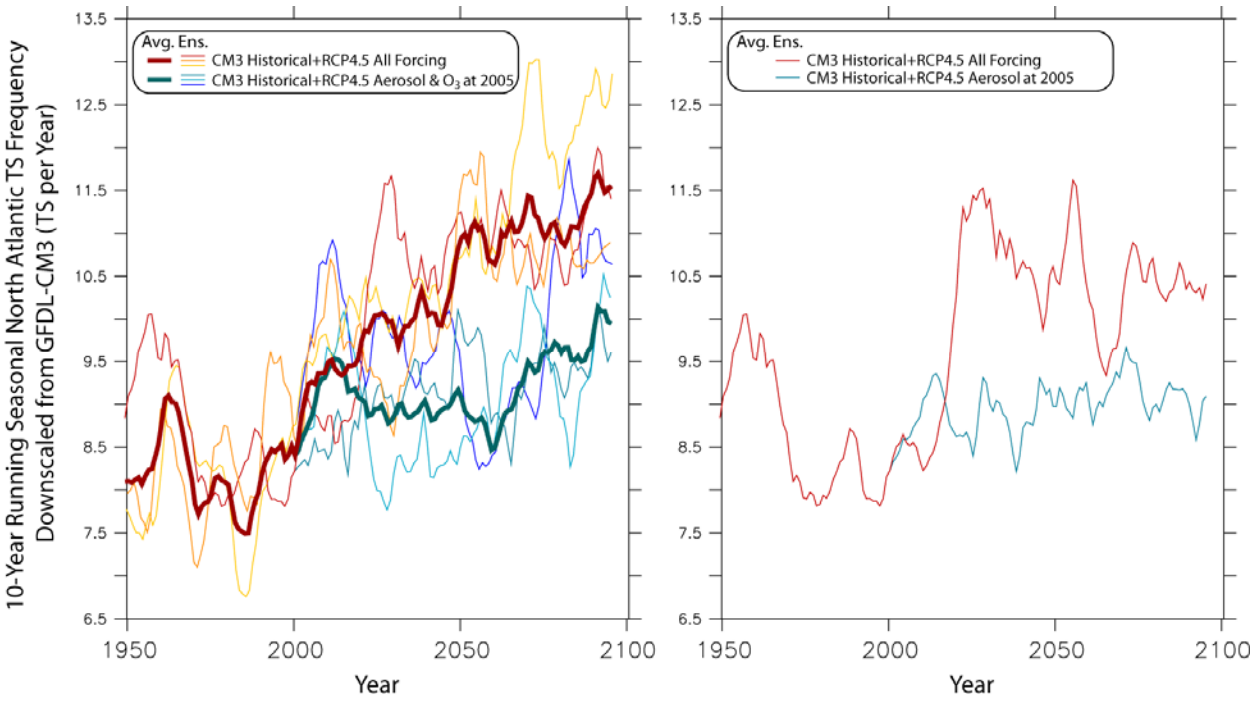

SUPPLEMENTARY FIGURE 4. Impact of future aerosol changes on North Atlantic Tropical Storm (NA TS) frequency projections using the GFDL-CM3 coupled model (Donner et al. 2011). Plotted is the ten-year centered average seasonal NA TS frequency downscaled using the methodology of Villarini et al (2010) based on the SST from a suite of experiments using the GFDL-CM3. In the left panel thin lines show two sets of three member ensembles, differing only in their initial conditions on 1-January-1860 (r1i1p1, r3i1p1 and r5i1p1 in the CMIP5 archive), and the thick lines show the three-member ensemble mean. The red lines show a combination of the "all forcing" historical runs and the projections for the 21st century under RCP4.5. Meanwhile, the blue lines show projections for the 21st century under RCP4.5, but with anthropogenic aerosol and CFC emissions held constant at their values for 2005. The difference between the two sets of lines indicates the impact of aerosols and GHGs (so stratospheric ozone) in the projections of GFDL-CM3 on NA TS frequency. Right hand panel shows an additional single ensemble member experiment couplet forced with the full historical and RCP4.5 forcing (red line) and with RCP4.5 except with aerosol emission held fixed at their 2005 levels after 2005 (blue line); the experiments on the right panel were run on a different computer than those in the left panel. These experiments together are consistent with aerosols being key to the projected increase in NA TS frequency for GFDL-CM3 under RCP4.5. Because similar experiments with the other GCMs used in the rest of this study (Supplementary Table 1) and with GFDL-CM3 for the other RCP scenarios are not available to us, we cannot confidently generalize this sensitivity to aerosol changes to other models. However, these results with a single model support the hypothesis in the main text that projected changes in anthropogenic aerosols are important to the projected NA TS increases in the CMIP5 model suite, and highlight the utility of idealized experiments to isolate forcing agents.

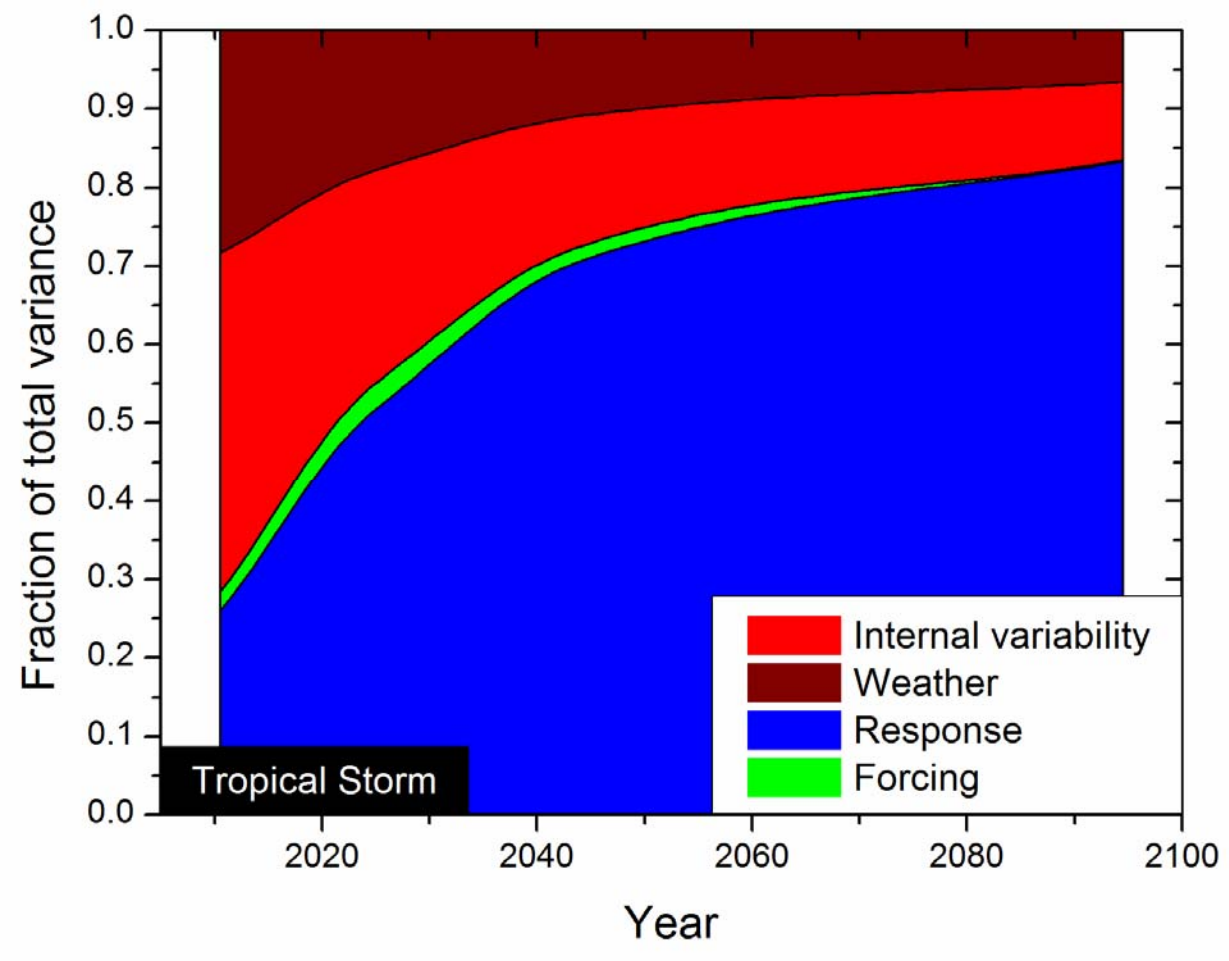

SUPPLEMENTARY FIGURE 5. Same as Figure 3d, but separating the contribution of "weather" and "internal variability" as defined in Hawkins and Sutton (2009).

Modeling Center (or Group)	Model Name	Historical	RCP 2.6	RCP 4.5	RCP 8.5	$2\times CO_2$
Beijing Climate Center, China Meteorological Administration	BCC-CSM1.1	Y	Y	Y	Y	Y
Canadian Centre for Climate Modelling and Analysis	CanESM2	Y	Y	Y	Y	Y
National Center for Atmospheric Research	CCSM4	Y	Y	Y	Y	Y
Centre National de Recherches Meteorologiques / Centre Europeen de Recherche et Formation Avancees en Calcul Scientifique	CNRM-CM5	Y	Y	Y	Y	Y
Commonwealth Scientific and Industrial Research Organization in collaboration with Queensland Climate Change Centre of Excellence	CSIRO-Mk3.6.0	Y	Y	Y	Y	Y
NOAA Geophysical Fluid Dynamics Laboratory	GFDL-CM3	Y	Y	Y	Y	Y
NOAA Geophysical Fluid Dynamics Laboratory	GFDL-ESM2M	Y	Y	Y	Y	Y
NOAA Geophysical Fluid Dynamics Laboratory	GFDL-ESM2G	Y	Y	Y	Y	Y
Met Office Hadley Centre	HadGEM2-ES	Y	Y	Y	Y	Y
Institut Pierre-Simon Laplace	IPSL-CM5A-LR	Y	Y	Y	Y	Y
Institut Pierre-Simon Laplace	IPSL-CM5A-MR	Y	Y	Y	Y	Y
Atmosphere and Ocean Research Institute (The University of Tokyo), National Institute for Environmental Studies, and Japan Agency for Marine-Earth Science and Technology	MIROC5	Y	Y	Y	Y	Y

Japan Agency for Marine-Earth Science and Technology, Atmosphere and Ocean Research Institute (The University of Tokyo), and National Institute for Environmental Studies	MIROC-ESM	Y	Y	Y	Y	Y
Japan Agency for Marine-Earth Science and Technology, Atmosphere and Ocean Research Institute (The University of Tokyo), and National Institute for Environmental Studies	MIROC-ESM-CHEM	Y	Y	Y	Y	-
Max Planck Institute for Meteorology	MPI-ESM-LR	Y	Y	Y	Y	Y
Meteorological Research Institute	MRI-CGCM3	Y	Y	Y	Y	Y
Norwegian Climate Centre	NorESM1-M	Y	Y	Y	Y	Y

SUPPLEMENTARY TABLE 1. Summary of the 17 global climate models used in this study. For all of them, data for the RCP 2.6, RCP 4.5 and RCP 8.5 are available. The same holds true for the $2\times CO_2$ runs with the exception of MIROC-ESM-CHEM.

REFERENCES

Donner, L.J. and co-authors. The dynamical core, physical parameterizations, and basic simulation characteristics of the atmospheric component AM3 of the GFDL Global Coupled Model CM3. *J. Climate*, **24**(13), DOI:10.1175/2011JCLI3955.1, (2011).

Jarvinen, B.R., C.J. Neumann, and M.A.S. Davis. A tropical cyclone data tape for the North Atlantic Basin, 1886–1983: Contents, limitations, and uses. NOAA Tech. Memo., NWS NHC 22 (1984)

Landsea, C.W., G.A. Vecchi, L. Bengtsson, and T.R. Knutson. Impact of duration thresholds on Atlantic tropical cyclone counts. *Journal of Climate* **23**, 2508–2519 (2010).

McAdie, C., C. Landsea, C.J. Neumann, J.E. David, and E.S. Blake. Tropical Cyclones of the North Atlantic Ocean, 1851–2006: With 2007 and 2008 Track Maps Included. 238 pp., Natl. Clim. Data Cent., Asheville, N. C. (2009).

Smith,T.M., R.W.Reynolds, T.C.Peterson, and J. Lawrimore. Improvements to NOAA's historical merged land–ocean surface temperature analysis (1880–2006). *Journal of Climate* **21**, 2283–2296 (2008).

Villarini, G., G.A. Vecchi, and J.A. Smith. Modeling of the dependence of tropical storm counts in the North Atlantic Basin on climate indices. *Monthly Weather Review* **138**(7), 2681–2705 (2010).